Available online at www.sciencedirect.com
ScienceDirect
Journal of Organometallic Chemistry 692 (2007) 2822–2831
Journal of Organometallic Chemistry
www.elsevier.com/locate/jorganchem

Ring and cage compounds from complexes of group 13 metal halides with ethylenediamine: Experiment and theory

C. Trinh, A.Y. Timoshkin *, S.M. Matveev, A.D. Misharev

Inorganic Chemistry Group, Department of Chemistry, St. Petersburg State University, Old Peterhoff, University Pr. 26, 198504 St. Petersburg, Russia

Received 15 October 2006; received in revised form 9 February 2007; accepted 9 February 2007
Available online 24 February 2007

Abstract

Formation of gaseous ring and cage compounds by thermolysis of the complexes between group 13 metal halides MX_3 and ethylenediamine (en) has been observed experimentally by mass spectrometry method (M = Al, Ga; X = Cl, Br, I) and studied theoretically. Existence of gaseous associates with molecular weight of 600–900 amu was observed for all studied systems. The abundance of the high molecular weight species decreases in order $AlBr_3 > AlI_3 > GaCl_3 > GaBr_3$. For aluminum compounds, formation of carbon-free cubane-type clusters was evidenced. Theoretical *ab initio* studies at B3LYP/LANL2DZ(d,p) level of theory have been performed for the series of the ring and cage oligomer compounds in Al_2Br_6-en system. A mechanistic pathway of the formation of inorganic rings and cages by subsequent HBr elimination and oligomerization reactions has been proposed. It is concluded that elimination reactions take place in the condensed phase.

Keywords: Group 13/15 compounds; Mass spectrometry; DFT calculations; Aluminum; Gallium; Inorganic rings and cages

1. Introduction

Binary nitrides of group 13 metals and ternary alloys $Al_xGa_{1-x}N$ are widely used as light emitting diodes and solar cell elements. Formation of composite nitrides with desired stoichiometric composition by chemical vapor deposition (CVD) method is a challenging task for chemists. To achieve this goal, single source precursors (SSP) which contain all necessary elements in desired stoichiometry ratio may be employed [1]. Among potential SSP, 13–15 ring and cage compounds and donor acceptor (DA) complexes of group 13 metal halides MX_3 with nitrogen containing polydentate ligands attracted some attention [2]. Existence of gaseous complexes of the type $MX_3 \cdot L\text{-}L \cdot MX_3$ (where bidentate donor ligand LL is 4,4′-bipyridine [3], tetramethylethylenediamine [4] and pyrazine [5]) was experimentally confirmed by mass spectrometry and tensimetry methods. Ethylenediamine $NH_2CH_2CH_2NH_2$ (en) is a well known chelating ligand, which with group 13 metal trications forms ionic complexes, for example $[Ga(en)_3]Cl_3$ [6]. However, en can potentially act as a bridging non-chelating ligand with formation of $MX_3 \cdot en \cdot MX_3$ complexes. Such complexes are known for the organoaluminum derivatives but have very low stability [7]. Formation of thermally unstable complexes of AlR_3 ($R = CH_3$, C_2H_5) with *N*,*N*-dimethylethylenediamine $NH_2(CH_2)_2N(CH_3)_2$ with 2:1 composition was proposed as a starting point towards amido complexes $AlR_3 \cdot NH(CH_2)_2NMe_2AlR_2$. Their pyrolysis at 190 °C results in formation of hexameric imido clusters $[RAlNCH_2CH_2NMe_2]_6$ [8]. Polymeric amides and imides were produced by pyrolysis of complexes of $AlMe_3 \cdot en \cdot AlMe_3$ and $AlEt_3 \cdot en \cdot AlEt_3$ [20]. Methane elimination and formation of dimeric amido complexes was evidenced in reaction of $Al(CH_3)_3$ with $NH_2CH_2(o\text{-}C_5H_4N)$ in hexane at 0 °C [9]. It is expected, that thermolysis of $MX_3 \cdot en \cdot MX_3$ complexes will result in hydrogen halide elimination and formation of ring and cage compounds. Chemistry of the ring and cage 13–15 compounds in the condensed phase have been reviewed

* Corresponding author.
E-mail address: alextim@at11692.spb.edu (A.Y. Timoshkin).

0022-328X/$ - see front matter © 2007 Elsevier B.V. All rights reserved.
doi:10.1016/j.jorganchem.2007.02.022

recently [10], however, there is a little information about their thermal stability in the gas phase. We suppose that substitution of the organometallic acceptors by group 13 metal halides will allow stabilization of the ring and cage compounds in the gas phase. Our previous theoretical studies of the thermolysis of the ammonia complexes $MX_3 \cdot NH_3$ [11,12] show that amido rings and imido cages are important intermediates in gas phase reactions In this report, we experimentally explore vapor composition over set of group 13 metal halide complexes ($MX_3 = AlBr_3$, AlI_3, $GaCl_3$, $GaBr_3$) with en. For the $AlBr_3$–en system, for which formation of the gas phase high mass species was found the most abundant, we also performed theoretical study of structures and stability of the ring and cage compounds.

2. Experimental

2.1. Computational details

GAUSSIAN 03 program package [13] was used throughout. All structures were fully optimized using density functional theory (DFT) with B3LYP [14,15] hybrid functional in conjunction with the effective core potential basis set LANL2DZ [16] augmented by d, p polarization functions as described in [17]. The previous study of complexes of 13 group metal halides with ammonia at B3LYP/LANL2DZ(d,p) level of theory showed satisfactory agreement with high temperature experimental data [17]. All reported structures are minima on the potential energy surface.

2.2. General remarks

Due to high air and moisture sensitivity all synthetic procedures were carried out in glass apparatus in a vacuum ($\sim 10^{-5}$ Torr). Group 13 metal halides were synthesized by direct interaction of metal with halogen and purified by multiple resublimations in vacuum. Purity control was performed by means of mass spectrometry and vapor pressure measurements.

Synthesis of complexes of 2:1 composition was performed by heating of slight excess of metal halide and en in sealed glass system under vacuum, excess of metal halide was removed by sublimation. Obtained products were studied by mass-spectrometry method using a standard MX-1321 mass spectrometer with direct probe introduction. The temperature of the ionization chamber was 200 °C, electron energy 70 eV, the temperature of sublimation chamber was varied from 120 to 430 °C.

3. Results and discussion

3.1. Mass spectrometry studies

Most important results of mass spectrometric studies are summarized in Table 1. Data clearly indicate presence of the pyrolytic processes. There are no peaks corresponding to the molecular complexes $M_2X_6en^+$, and only for the $GaCl_3 \cdot en \cdot GaCl_3$ system daughter ion $M_2X_5en^+$ was detected at low (220 and 270 °C) temperatures, at higher temperatures this ion was not present. This indicate existence of the complex of 2:1 composition $GaCl_3 \cdot en \cdot GaCl_3$ only at low temperatures. Similar situation was recently observed for mass spectra of the $GaCl_3 \cdot pyz \cdot GaCl_3$ system (pyz, pyrazine), where existence of the complex of 2:1 was confirmed by tensimetric studies [5]. Presence of the ions $MX_2NHCH_2CH_2NH_2MX_2^+$ with high intensity indicates HX elimination as a primary destruction process of the MX_3enMX_3.

It is noteworthy that presence of the species with high molecular weigh was detected for all samples at temperature interval 270–380 °C. The abundance (number of different species and their relative intensity) of the high molecular weight ions decreases in order $AlBr_3 > AlI_3 > GaCl_3 > GaBr_3$. For gallium containing systems, only a few peaks of very low intensity have been detected. Only selected high molecular weight peaks are presented in Table 1. We also note that in case of gallium compounds, GaX_3^+ ions have been detected, while they are absent in case of aluminum compounds. We attribute the appearance of the GaX_3^+ ions to the partial dissociation of the gallium-containing adducts. This observation dovetails with lower (by about 30 kJ mol^{-1}) Ga–N bond energy in the donor–acceptor complexes $GaX_3 \cdot en$ and $GaX_3 \cdot en \cdot GaX_3$ compared to their aluminum counterparts [18].

Among the cluster species, ions $M_3X_4C_4N_4H_{12}^+$ have the highest intensity, their existence was registered in MS up to 430 °C. For the $AlBr_3{\cdot}en{\cdot}AlBr_3$ system, we report mass spectra of the initial sample after the synthesis and (in parenthesis) of the sublimate after thermal treatment (circa 8 days at 220–250 °C). As can be seen, after such thermal treatment relative intensities of the cluster species $M_3X_4C_4N_4H_{12}^+$ and $M_3X_5C_4N_4H_{12}^+$ have increased (ion $M_3X_4C_4N_4H_{12}^+$ becomes the most intensive), and formation of carbon-free clusters with four aluminum atoms $Al_4X_4N_4H_4^+$, was evidenced. Similar situation (highest intensity of $M_3X_4C_4N_4H_{12}^+$ and presence of carbon-free $Al_4X_4N_4H_4^+$) is observed for the $AlI_3 \cdot en \cdot AlI_3$ complex even without additional thermal treatment. This indicates, that pyrolysis proceeds easier for the AlI_3 compared to $AlBr_3$. Prolonged heating of the samples at ~350 °C resulted in complete decomposition (no aluminum-containing ions were observed in the mass spectrum).

Thus, we conclude that thermal destruction of the complexes of group 13 metal halides with en of 2:1 composition is accompanied by formation of high molecular weight species. To get further insight into structures and stability of these species, quantum chemical calculations have been performed for the system $AlBr_3 \cdot en \cdot AlBr_3$ for which the maximal variety of the cluster species have been observed experimentally.

Table 1
Mass spectra of complexes of aluminum and gallium halides with en (70 eV)

Ion	Proposed structure	Relative intensity *I*, (%)				
		$Al_2Br_6 \cdot en$[a]		$Al_2I_6 \cdot en$[a]	$Ga_2Cl_6 \cdot en$[b]	$Ga_2Br_6 \cdot en$[b]
CNH_4^+	$CH_2NH_2^+$	100	(93.4)	87.5	100	84.6
$C_2N_2H_8^+$	$NH_2CH_2CH_2NH_2^+$	9.0	(6.1)	2.5	27.3	22.8
$MN_2C_2H_6^+$	$MNCH_2CH_2NH_2^+$ (**I** minus X)$^+$	35.0	(43.7)	21.4	5.5	3.9
MX^+	MX^+	–	(–)	–	11.6	15.4
MX_2^+	MX_2^+	14.0	(20.3)	5.3	34.9	100
MX_3^+	MX_3^+	–	(–)		5.6	39.0
$MXC_2N_2H_5^+$	$MXNCH_2CH_2NH^+$	55.0	(71.6)	17.8	–	–
$MXC_2N_2H_7^+$	$MXNHCH_2CH_2NH_2^+$	–	(–)	–	57.0	28.5
$MX_2C_2N_2H_6^+$	$MX_2NHCH_2CH_2NH^+$	8.0	(31.1)	1.1	–	–
$MX_2C_2N_2H_7^+$	$MX_2NH_2CH_2CH_2NH^+$ ($_{ring}$**A**)$^+$	27.8	(9.3)	0.8	17.2	–
$MX_2C_2N_2H_8^+$	$MX_2NH_2CH_2CH_2NH_2^+$ (**C** minus X)$^+$	–	(–)	–	21.9	35.8
$M_2X_2C_2N_2H_6^+$	$MXHNCH_2CH_2NMX^+$ (**AI** minus X)$^+$	14.8	(23.4)	6.4	–	–
$M_2X_3C_2N_2H_6^+$	$MX_2NHCH_2CH_2NHMX^+$ ($_{ring}$**AA** minus X)$^+$	37.0	(55.3)	3.9	–	–
$M_2X_4C_2N_2H_7^+$	$MX_2NHCH_2CH_2NH_2MX_2^+$ ($_{ring}$**CA** minus X)$^+$	15.3	(18.4)	–	59.6	31.8
$M_2X_5C_2N_2H_7^+$	$MX_2NHCH_2CH_2NH_2MX_3^+$($_{ring}$**CA**)$^+$	–	(–)	–	–	1.9
$M_2X_5C_2N_2H_8^+$	$MX_2NH_2CH_2CH_2NH_2MX_3^+$(**CC** minus X)$^+$	–	(–)	–	0.6	–
$M_4X_4N_4H_4^+$	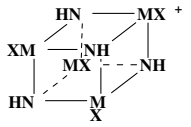	–	(7.2)	2.9	–	–
$M_3X_4C_4N_4H_{12}^+$	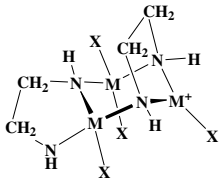	72.0	(100)	100	–	–
$M_3X_5C_4N_4H_{12}^+$	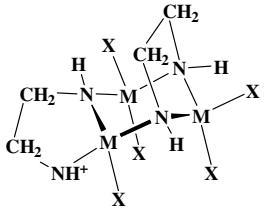	33.8	(48.1)	0.2	–	–
$M_3X_5C_4N_4H_{13}^+$	(**AA_A** minus X)$^+$	20.3	(24.1)	–	–	–

Relative intensities *I* with respect to the most intensive ion. Data in parenthesis are for the sample after the thermal treatment. See text for details.
[a] T = 380 °C.
[b] T = 270 °C.

3.2. Theoretical studies of stability of ring and cage compounds

In order to systematically approach the question of formation of high molecular weight species upon hydrogen halide elimination, we considered scheme of the subsequent HBr elimination from two sets of molecular complexes, $AlBr_3 \cdot en$ (1:1 composition) and $AlBr_3 \cdot en \cdot AlBr_3$ (2:1 composition) and oligomerization of the obtained products (Scheme 1). In this paper, we will use the following notation: single letter notation refers to compounds with one metal center (1:1 composition): **C** indicates donor–acceptor complex $AlBr_3 \cdot en$, **A** indicates monomeric amido compound $AlBr_2NHCH_2CH_2NH_2$; **I** indicates monomeric imido compound $AlBrNCH_2CH_2NH_2$. Their respective oligomers with oligomerization degree *n* are indicated $\mathbf{A_n}$ and $\mathbf{I_n}$. Similarly, two letter notation refers to compounds with 2:1 composition: **CC** indicates donor–acceptor complex $AlBr_3 \cdot en \cdot AlBr_3$, **CA** indicates complex–amido compound $AlBr_3NH_2CH_2CH_2NHAlBr_2$, **AA** indicates amido–amido compound $AlBr_2NHCH_2CH_2NHAlBr_2$; **AI** indicates amido–imido compound $AlBr_2NHCH_2CH_2NAlBr$; **II** indicates imido–imido compound $AlBrNCH_2CH_2NAlBr$. Their respective oligomers are labeled $\mathbf{AA_n}$, $\mathbf{AI_n}$, $\mathbf{II_n}$. In the present report, we will focus our attention on the reactions leading to the experimentally observed amido species. At first, we will

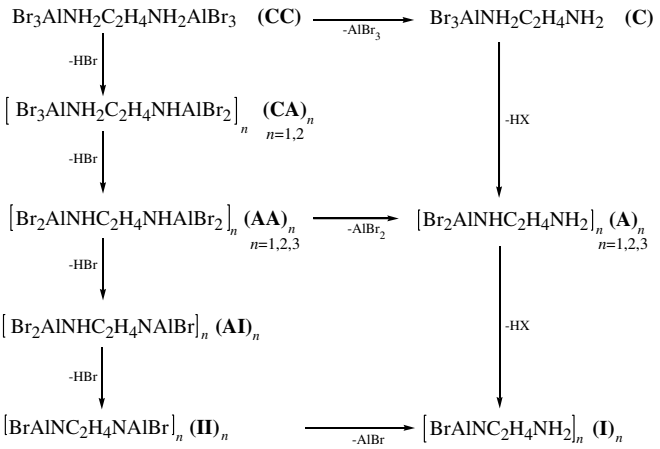

Scheme 1. General scheme for the decomposition processes of $AlBr_3$-e-n$AlBr_3$ complex and compound labeling.

discuss structures, relative energies and reaction energetics for the monomeric amido compounds. After that we will turn our attention to the formation of the most dominant oligomeric amido compounds.

3.2.1. Structures and relative energetics of monomeric amido compounds

Optimized structures of the source DA complexes **C** and **CC** are presented in Fig. 1a and b, and those of the two isomers of monomeric amido compounds **A** of 1:1 composition are given in Fig. 1c and d. Ring isomer $_{ring}$**A** (Fig. 1c) is by 107 kJ mol^{-1} more stable compared to the chain isomer $_{chain}$**A** (Fig. 1d). Both isomers possess a nitrogen atom with low coordination number 3 and can form DA complexes with $AlBr_3$. Optimized structures of such **CA** compounds are presented in Figs. 1e and f. Complexation of $AlBr_3$ with $_{ring}$**A** (presence of the $AlBr_2$ moiety directly attached to the complexing nitrogen) is less favorable compared to complexation with $_{chain}$**A** ($AlBr_2$ moiety is quite remote and does not affect complexing). The energy difference between the $_{ring}$**CA** (Fig. 1e) and $_{chain}$**CA** (Fig. 1f) is 98 kJ mol^{-1} in favor of the ring isomer. Hydrogen halide elimination from **CA** can lead either to **CI** or **AA** compounds; our previous results [18] show that formation of amido–amido compounds **AA** is more favorable by about 200 kJ mol^{-1}. Therefore, we will not discuss **CI** structures in the present report. Three isomers of **AA** were considered. Ring isomer $_{ring}$**AA** (Fig. 1g) is by 147 kJ mol^{-1} more stable than respective chain isomer $_{chain}$**AA** (Fig. 1h). Alternative ring structure with bridging bromine atoms $_{ring\_br\_}$**AA** (Fig. 1i) is by 130 kJ mol^{-1} higher in energy compared to $_{ring}$**AA**. Thus, among considered structures, computational results clearly show preference of the ring isomers of **A** and **AA**.

3.2.2. Reaction energetics of the formation of monomeric amido compounds

There are two major decomposition pathways for the $AlBr_3 \cdot en \cdot AlBr_3$ complex: (1) thermal dissociation into

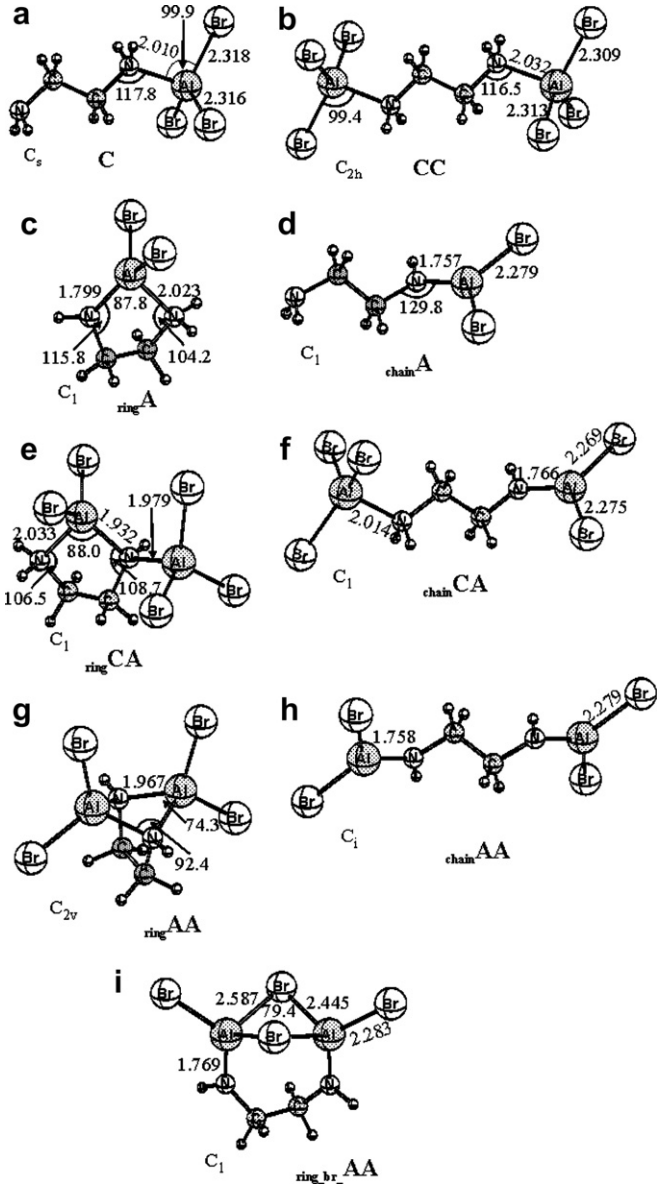

Fig. 1. Optimized structures of source donor–acceptor complexes and monomeric amido compounds. (a) $AlBr_3$en (**C**); (b) $AlBr_3 \cdot en \cdot AlBr_3$ (**CC**); (c) ring isomer of monomeric amido compound ($_{ring}$**A**); (d) chain isomer of monomeric amido compound ($_{chain}$**A**); (e) donor–acceptor complex of the ring isomer of monomeric amido compound ($_{ring}$**CA**); (f) donor–acceptor complex of the chain isomer of monomeric amido compound ($_{chain}$**CA**); (g) ring isomer of monomeric amido compound with Al_2N_2 core ($_{ring}$**AA**); (h) chain isomer of monomeric amido compound ($_{chain}$**AA**); (i) ring isomer of monomeric amido compound with Al_2Br_2 core ($_{ring\_br\_}$**AA**). All distances in Å, all angles in °. B3LYP/LANL2DZ(d,p) level of theory.

components and (2) HBr elimination reactions. To address the possibility of formation of $_{ring}$**A**, $_{ring}$**CA**, and $_{ring}$**AA** from $AlBr_3 \cdot en \cdot AlBr_3$ we should take into account concurrence between these two pathways. For our thermodynamic analysis, we will use the value of the temperature, at which the equilibrium constant of the respective process equals one ($T_{K=1}$). This single criterion takes into account both enthalpy and entropy factors, and its value can be estimated as $T_{K=1} \approx \Delta H^{\circ}_{298}/\Delta S^{\circ}_{298}$. Such approximation

was found to produce satisfactory agreement with experimental results for the MX_3-ammonia complexes [17].

Predicted thermodynamic characteristics of the initial thermal destruction processes are summarized in Table 2. As follows from the comparison of $T_{K=1}$ values, HBr elimination from $AlBr_3 \cdot en \cdot AlBr_3$ with formation of $_{ring}$**CA** (process 2) is expected to start at lower temperatures, compared to its dissociation into $AlBr_3 \cdot en$ (process 1). However, elimination of the second HBr molecule is more demanding energetically, and $_{ring}$**CA** should rather dissociate into $_{ring}$**A** and $AlBr_3$ (process 3) than form a monomeric amido–amido $_{ring}$**AA** (reaction 4). Note also, that if $AlBr_3 \cdot en$ complex is formed by reaction 1, HBr elimination with formation of $_{ring}$**A** (process 6) is also expected at much lower temperatures compared to dissociation of $AlBr_3 \cdot en$ into components (process 5). Process 2 has the lowest value of $T_{K=1}$ (763 K), followed by processes **6** (817 K), **1** (825 K) and **3** (860 K). Thus, it appears that $_{ring}$**CA** compound, formed by reaction 2, is one of the expected initial products. Our theoretical conclusions are in accord with results observed by mass spectrometry. Indeed, presence of daughter ions of $_{ring}$**CA**, namely $Al_2Br_4N_2C_4H_7^+$ ($_{ring}$**CA**$^+$ minus Br) was observed in mass-spectrum. We also note, that $M_2X_4N_2C_4H_7^+$ ions are present for all but Al_2I_6en system, which indicates common decomposition pathway for all studied complexes. The absence of ions related to monomeric **CA** compound in case of Al_2I_6en can be explained on the basis that its further decomposition proceeds much easier, in part due to higher favorability of HI elimination reactions in the aluminum iodine–en system [18].

Our thermodynamic analysis also shows, that formation of $_{ring}$**A** compound $AlBr_2N_2C_2H_7$ by sequence of processes 1 and 6, (or, alternatively, 2 and 3) is also expected thermodynamically. Indeed, corresponding ions $AlBr_2N_2C_2H_7^+$ are present in mass-spectra. Thus, our computations show that in the gas phase HBr elimination with formation of ring isomers of monomeric amido compounds $_{ring}$**A** and $_{ring}$**CA** should take place before the dissociation of the donor–acceptor bond. However, predicted decomposition temperatures for the gas phase reactions (about 500 °C) are much higher compared to the observed decomposition temperatures. We believe that decomposition reactions start already in the condensed phase after the melt of the complexes. We also note that due to high volatility of HBr, its evolution from the condensed phase is expected to facilitate HBr elimination reactions due to favorable entropy factor.

We conclude both from experimental and theoretical results, that $_{ring}$**A** and $_{ring}$**CA** compounds are the primary products in the decomposition pathway of the donor–acceptor complex $AlBr_3 \cdot en \cdot AlBr_3$. These key initial compounds can undergo further reactions. Since the Al–N bond in amido compounds is very strong (~380–415 kJ mol^{-1} [18]), reactions with dissociation of this bond are not expected. We suggest that further HBr elimination reactions from $_{ring}$**A** and $_{ring}$**CA** and oligomerization of the obtained products may occur. Therefore, stability of the oligomers with respect to dissociation into the ring monomers becomes an important issue.

3.2.3. Structures, relative energies and stability of oligomeric amido compounds

Dimerization of ring isomer of amido compound $_{ring}$**A** with itself is not possible, since Al center has already achieved favorable coordination number four. On the contrary, chain isomer $_{chain}$**A** possess unsaturated Al and N centers and can dimerize in different fashions. Optimized structures of three considered isomers of $\mathbf{A_2}$ are presented in Figs. 2a–c. The most stable isomer $\mathbf{A_{2a}}$ (Fig. 2a) has planar Al_2N_2 ring with *trans*-orientation of organic substituents $–C_2H_4NH_2$ with respect to the Al_2N_2 plane. Corresponding $\mathbf{A_{2c}}$ isomer with *cis*-orientation of organic substituents (Fig. 2c) lies 35 kJ mol^{-1} higher in energy. Alternative $\mathbf{A_{2b}}$ structure with 10-membered non-planar $Al_2N_4C_4$ cycle (Fig. 2b) is by 18 kJ mol^{-1} higher in energy compared to $\mathbf{A_{2a}}$. Dissociation of the $\mathbf{A_{2a}}$ compound into $_{ring}$**A** is only slightly endothermic (33 kJ per mole of $\mathbf{A_2}$) but favorable by entropy (157 J mol^{-1} K^{-1}). This leads to negative values of the standard Gibbs energy for the dissociation process above 210 K, therefore dimers of amido compounds are not stable with respect to dissociation into monomers even at room temperature.

Dimerization of the $_{ring}$**CA** with itself is also impossible, but $_{chain}$**CA** readily dimerizes to form $\mathbf{CA_2}$ (Fig. 1d) which features central Al_2N_2 ring. Dimerization of $_{chain}$**CA** is quite exothermic (212 kJ per mol of $\mathbf{CA_2}$), however, if dimerization of $_{ring}$**CA** is considered, the reaction is exothermic only by 19 kJ mol^{-1} and unfavorable by entropy by 128 J mol^{-1} K^{-1}. This leads to the instability of the

Table 2
Thermodynamic characteristics of the initial gas phase reactions of $AlBr_3 \cdot en \cdot AlBr_3$ complex dissociation and HBr elimination processes with formation of monomeric amido compounds

N	Process	ΔH°_{298} (kJ mol^{-1})	ΔS°_{298} (J mol^{-1} K^{-1})	$T_{K=1}$ (K)
1	$AlBr_3 \cdot en \cdot AlBr_3 = AlBr_3 \cdot en + AlBr_3$	129.6	157.2	825
2	$AlBr_3 \cdot en \cdot AlBr_3 =$ $_{ring}$**CA**+HBr	83.6	109.5	763
3	$_{ring}$**CA** = $_{ring}$**A**+$AlBr_3$	142.3	165.5	860
4	$_{ring}$**CA** = $_{ring}$**AA**+HBr	148.9	107.9	1380
5	$AlBr_3 \cdot en = AlBr_3$+en	155.1	143.4	1082
6	$AlBr_3 \cdot en =$ $_{ring}$**A**+HBr	96.3	117.9	817

B3LYP/LANL2DZ(d,p) level of theory.

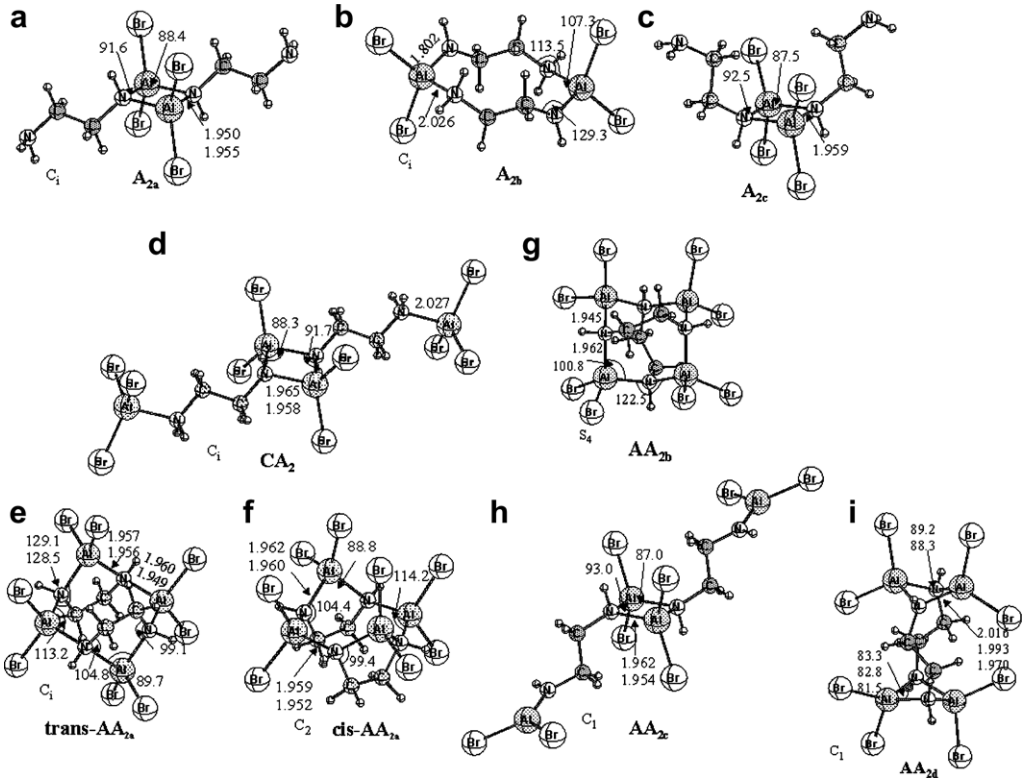

Fig. 2. Optimized structures of dimeric amido compounds. (a) $\mathbf{A_{2a}}$; (b) $\mathbf{A_{2b}}$; (c) $\mathbf{A_{2c}}$; (d) $\mathbf{CA_2}$; (e) *trans*-$\mathbf{AA_{2a}}$; (f) *cis*-$\mathbf{AA_{2a}}$; (g) $\mathbf{AA_{2b}}$; (h) $\mathbf{AA_{2c}}$; (i) $\mathbf{AA_{2d}}$. All distances in Å, all angles in °. B3LYP/LANL2DZ(d,p) level of theory.

$\mathbf{CA_2}$ dimer with respect to dissociation into $_{\mathbf{ring}}\mathbf{CA}$ monomer above 150 K.

Following Jiang and Interrante [20], for the amido polymers $\mathbf{AA_n}$ two sets of structures can be suggested, one featuring five-member AlN_2C_2 ring (Scheme 2a) and another one based on the four-member Al_2N_2 ring (Scheme 2b). We considered five isomers of $\mathbf{AA_2}$ compounds, their optimized structures presented in Figs. 2e–i. The most stable isomer *trans*-$\mathbf{AA_{2a}}$ ($\mathbf{C_i}$ point group, Fig. 2e) features two five-member AlN_2C_2 rings (with opposite orientation against each other) bridged together by two $AlBr_2$ groups. The isomer with sin-orientation of the five-member AlN_2C_2 rings *cis*-$\mathbf{AA_{2a}}$ (C_2 point group, Fig. 2f) lies 38 kJ mol^{-1} higher in energy. Alternative structure with seven-member rings $Al_2N_3C_2$ $\mathbf{AA_{2b}}$ (S_4 point group, Fig. 2g) lies 52 kJ mol^{-1} higher in energy. Dimeric structures based on Al_2N_2 ring motif are much less stable. Isomer $\mathbf{AA_{2c}}$ (Fig. 2h) with perfectly planar Al_2N_2 core and unsaturated terminal $AlBr_2$ groups lies 216 kJ mol^{-1} higher in energy. Attempt to close this isomer with formation of two Al_2N_2 rings joined together by two $-CH_2CH_2-$ bridges results in loss of planarity of the Al_2N_2 rings due to high steric demands, optimized structure $\mathbf{AA_{2d}}$ (Fig. 2i) is 247 kJ mol^{-1} higher with respect to the most stable isomer. Dissociation of the most stable *trans*-$\mathbf{AA_{2a}}$ into two $_{\mathbf{ring}}\mathbf{AA}$ is endothermic by 126 kJ mol^{-1}, but favored by entropy (172 J mol^{-1} K^{-1}). Existence of *trans*-$\mathbf{AA_{2a}}$ dimer is expected at temperatures below 730 K (which is lower compared to the temperatures required for the generation of $_{\mathbf{ring}}\mathbf{AA}$). Therefore, existence of the dimeric forms of amido–amido compounds in the gas phase appears to be unfavorable.

We also considered possibility of further oligomerization by taking into account trimeric amido compounds. Their optimized structures are given in Fig. 3. For $\mathbf{A_3}$, two isomers based on Al_3N_3 ring have been considered. More symmetric isomer $\mathbf{A_{3a}}$ with *cis*-orientation of organic substituents (C_3 point group) is marginally (by 3.4 kJ mol^{-1}) more stable compared to C_s symmetric isomer $\mathbf{A_{3b}}$. Dissociation of $\mathbf{A_3}$ into $_{\mathbf{ring}}\mathbf{A}$ is endothermic only by 5.6 kJ mol^{-1}, and very favorable by entropy (334 J mol^{-1} K^{-1}).

For $\mathbf{AA_3}$, five isomers have been considered. In agreement with our findings for amido–amido dimers, the most stable isomer $\mathbf{AA_{3a}}$ (Fig. 3c) possess structure based on five-member ring AlN_2C_2 motif, three such rings bridged via $AlBr_2$ groups. Structures based on four-member

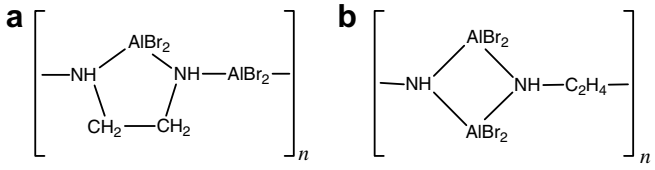

Scheme 2. Construction of $\mathbf{AA_n}$ oligomers based on five-member AlN_2C_2 ring (a) and four-member Al_2N_2 ring (b) according to Jiang and Interrante [20].

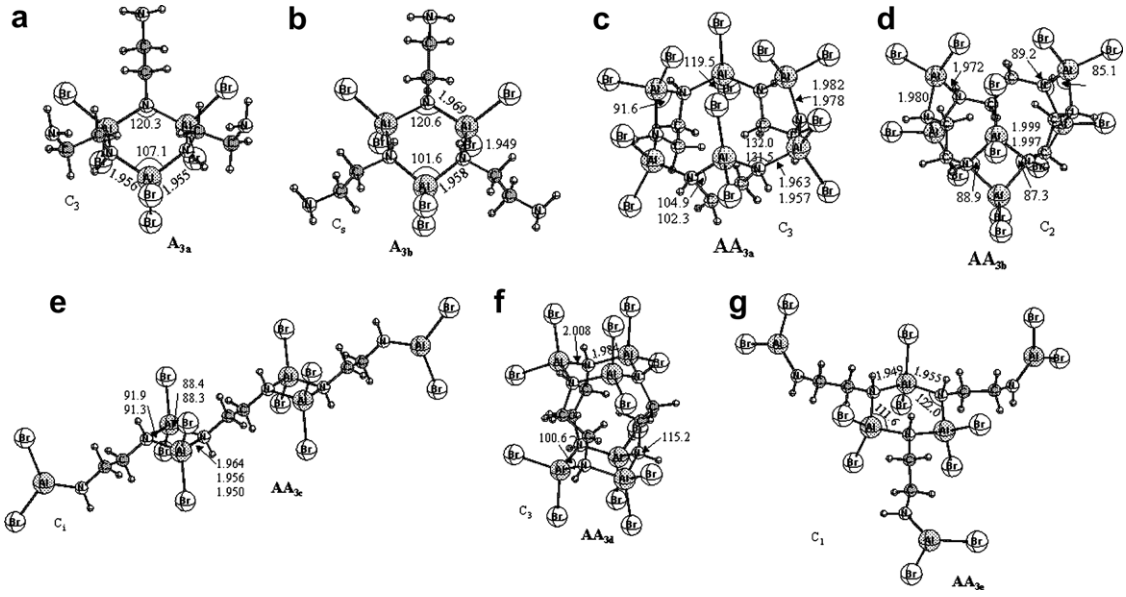

Fig. 3. Optimized structures of trimeric amido compounds. (a) $\mathbf{A_{3a}}$; (b) $\mathbf{A_{3b}}$; (c) $\mathbf{AA_{3a}}$; (d) $\mathbf{AA_{3b}}$; (e) $\mathbf{AA_{3c}}$; (f) $\mathbf{AA_{3d}}$; (g) $\mathbf{AA_{3e}}$. All distances in Å, all angles in °. B3LYP/LANL2DZ(d,p) level of theory.

Al_2N_2 rings bridged by C_2H_4 groups are higher in energy. We considered two such structures, the first one is closed cyclic structure $\mathbf{AA_{3b}}$ (Fig. 3d), where all three Al_2N_2 rings bridged together by C_2H_4 groups forming a closed cycle. This structure lies by 103 kJ mol^{-1} higher in energy compared to the most favorable structure $\mathbf{AA_{3a}}$. The second structure $\mathbf{AA_{3c}}$ (Fig. 3e) has only two Al_2N_2 rings with unsaturated $AlBr_2$ groups at the end. It can be considered as open $\mathbf{AA_{3b}}$ cycle. $\mathbf{AA_{3c}}$ is by 105 kJ mol^{-1} higher in energy compared to $\mathbf{AA_{3a}}$. This small (only 2 kJ mol^{-1}) difference between open-end $\mathbf{AA_{3c}}$ and closed-end $\mathbf{AA_{3b}}$ indicates that despite the attaining the favorable coordination number 4 upon cyclization, the strain in the trimeric cycle $\mathbf{AA_{3b}}$ is still significantly large.

We also considered two isomers with structures based on six-member Al_3N_3 rings: $\mathbf{AA_{3d}}$ featuring two such rings bridged together by C_2H_4 groups (Fig. 3f) and $\mathbf{AA_{3e}}$ featuring one Al_3N_3 ring with three open-end $AlBr_2$ groups (Fig. 3g). These isomers are higher in energy with respect to $\mathbf{AA_{3a}}$ by 227 and 253 kJ mol^{-1}, respectively.

Our computational results both for dimers and trimers suggest that isomers based on the five-member AlN_2C_2 ring

Table 3
Gas phase thermodynamic characteristics for the dissociation of oligomeric compounds into the ring monomers (per one mole of monomer)

Process	ΔH°_{298} (kJ mol^{-1})	ΔS°_{298} (J mol^{-1} K^{-1})	ΔG°_{298} (kJ mol^{-1})	$T_{K=1}$ (K)
½ $\mathbf{A_2} = {}_{\mathbf{ring}}\mathbf{A}$	16.3	78.3	−7.0	209
⅓ $\mathbf{A_3} = {}_{\mathbf{ring}}\mathbf{A}$	1.8	110.9	−31.3	17
½ $\mathbf{CA_2} = {}_{\mathbf{ring}}\mathbf{CA}$	9.7	64.0	−9.4	151
½ *trans*-$\mathbf{AA_{2a}} = {}_{\mathbf{ring}}\mathbf{AA}$	37.3	86.1	37.4	732
⅓ $\mathbf{AA_{3a}} = {}_{\mathbf{ring}}\mathbf{AA}$	46.5	109.8	13.7	423

B3LYP/LANL2DZ(d,p) level of theory.

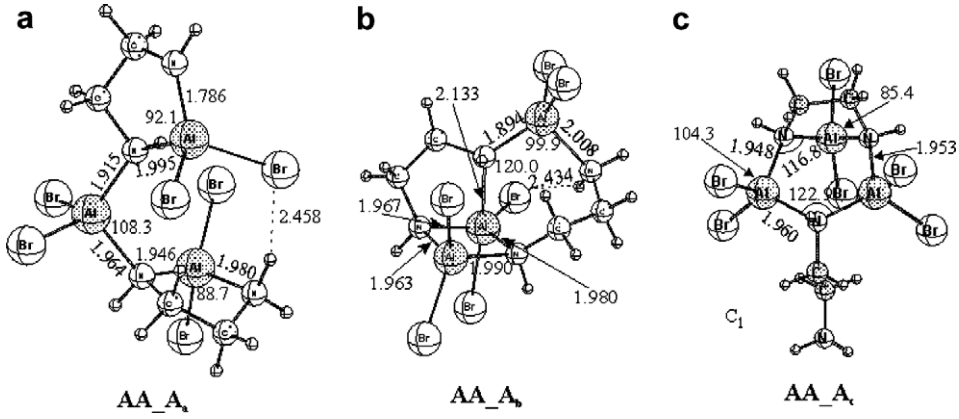

Fig. 4. Optimized structures of the $Al_3Br_6C_4N_4H_{13}$ isomers. (a) $\mathbf{AA\_A_a}$; (b) $\mathbf{AA\_A_b}$; (c) $\mathbf{AA\_A_c}$. All distances in Å, all angles in °. B3LYP/LANL2DZ(d,p) level of theory.

(Scheme 2a) are more stable compared to those based on four-member Al_2N_2 ring (Scheme 2b). However, the instability of the isomers based on four-member Al_2N_2 ring motif is largely due to unfavorable strain in closing the structure. As the oligomerization degree n increases, strain induced by bridging Al_2N_2 rings with $–C_2H_4–$ groups is expected to decline. In fact, for $n = 2$ the energy difference between the isomers is 247 kJ mol^{-1} in favor of five-member ring motif, while for $n = 3$ the energy difference reduces to only 103 kJ mol^{-1}. Projection of this trend lead us to conclusion that Al_2N_2-based polymers could have comparable stability with polymers based on five-member AlN_2C_2 rings.

Summarizing our findings for the stability of amido and amido–amido oligomers, Table 3 provides thermodynamic characteristics of their dissociation computed per mole of monomer. Both in amido and amido–amido series stability of the oligomers decreases with an increase of the oligomerization degree n. Most of the dimers and trimers are not stable even at room temperature, the notable exception is *trans*-$\mathbf{AA_{2a}}$ dimer which is predicted to be stable up to 730 K.

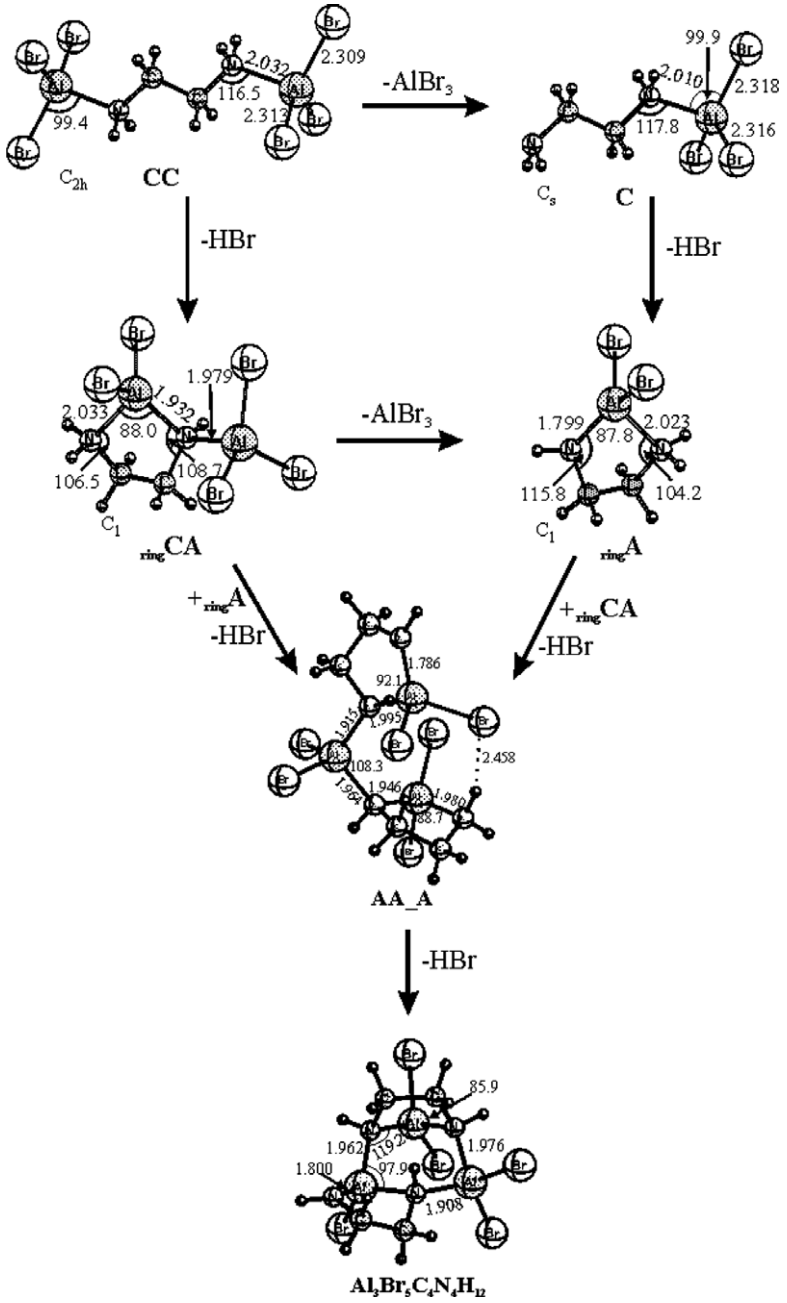

Fig. 5. Scheme of the gas phase reactions leading to the experimentally observed oligomer species. Structures of the most stable isomer for the each composition are shown. All distances in Å, all angles in °. B3LYP/LANL2DZ(d,p) level of theory.

Table 4
Thermodynamic characteristics of the gas phase reactions leading to experimentally observed oligomer compounds

N	Process	ΔH°_{298} (kJ mol^{-1})	ΔS°_{298} (J mol^{-1} K^{-1})	$T_{K=1}$ (K)
7	$_{ring}$**CA** + $_{ring}$**A** = **AA_A** + HBr	52.1	−64.0	–
8	**AA_A** = $Al_3Br_5C_4N_4H_{12}$ + HBr	143.0	125.0	1143
9	CC + C = $Al_3Br_5C_4N_4H_{12}$ + 4HBr	375.0	288.4	1300
10	**CC** = $^1/_2$ $[BrAlNH]_4$ + $C_2H_4Br_2$ + 2HBr	326.9	300.5	1088
11	**CC** = $^1/_2[BrAlNH]_4$ + C_2H_2 + 4HBr	543.9	572.8	950
12[a]	**CC** = $^1/_2[BrAlNH]_4$ + $2C_{(solid)}$ + H_2 + 4HBr	317.2	515.0	616

B3LYP/LANL2DZ(d,p) level of theory.
[a] Values for this reaction are obtained from reaction **11** using thermodynamic parameters of C_2H_2 (g), C (s) and H_2(g) taken from Ref. [22].

3.2.4. Structures and reaction energetics of the experimentally observed oligomer compounds

As can be seen from Table 1, we experimentally observe in large quantities species consistent with three aluminum atoms and two en units. Formation of such compounds may be attributed to the reaction between the most stable monomeric compounds $_{ring}$**CA** and $_{ring}$**A** with elimination of 1 mole of HBr. Resulting compound formally is a combination of 2:1 and 1:1 amido monomers, it will be denoted as **AA_A**. Three isomers of this compound have been considered, the most stable is **AA_Aa** based on two five-member AlN_2C_2 rings bridged by $AlBr_2$ (Fig. 4a). Alternative structures **AA_Ab** (Fig. 4b) and **AA_Ac** (Fig. 4c) are by 10 and 27 kJ mol^{-1} higher in energy. Although molecular ion of **AA_A** was not detected by mass spectrometry, the daughter ion (**AA_A** minus Br)$^+$ was observed. Compound **AA_A** exhibit relatively short intramolecular H···Br distance (2.46 Å for **AA_Aa** and 2.43 Å for **AA_Ab**) and can further eliminate HBr with formation of $Al_3Br_5C_4N_4H_{12}$. Both molecular and daughter ions of $Al_3Br_5C_4N_4H_{12}$ are detected in the mass-spectrum, and the daughter ion ($Al_3Br_5C_4N_4H_{12}$ minus Br)$^+$ has the highest intensity for the sample after prolonged thermal heating. Thus, processes leading to formation of experimentally observed high mass species can be summarized by reaction sequence shown in Fig. 5. Thermodynamic characteristics of these reactions are given in Tables 2 and 4. As follows from our thermodynamic analysis, formation of gaseous **AA_A** from gaseous $_{ring}$**CA** and $_{ring}$**A** (process 7) is thermodynamically forbidden at all temperatures. Temperatures, at which gas phase reactions 8 and 9 are expected to operate are too high (above 1100 K). However, HBr elimination reactions in the condensed phase are expected to be favorable by entropy and proceed at much lower temperatures.

It is also interesting to address the thermodynamics of formation of carbon-free oligomer species $Al_4X_4N_4H_4$. These species are formed only after a prolonged heating in case of Al_2Br_6en, but for Al_2I_6en such clusters were detected even without additional thermal treatment. The most probable structure is a cubane-type imido tetramer, analogs of which are well-known experimentally [10]. $[XMNH]_n$ oligomers have been also studied before theoretically [21]. We explored gas phase reactions toward formation of $Al_4Br_4N_4H_4$ from the donor–acceptor complex $AlBr_3 \cdot en \cdot AlBr_3$. Achieving of carbon-free cubane requires complete removal of the organic substituents. We considered three possible processes, with formation of gaseous HBr and $C_2H_2Br_2$; HBr and C_2H_2; and H_2, HBr and solid carbon as by-products (processes 10–12 in Table 4). All reactions are endothermic but favorable by entropy, thus they are expected to operate at high temperatures. The reaction with formation of solid carbon, hydrogen and HBr (process 12) proceeds at much lower temperatures compared to processes 10 and 11 and is expected to operate around 340 °C. Thus, our analysis shows that formation of carbon-free cubanes is thermodynamically allowed at high (around 340 °C) temperatures. This theoretical conclusion supports our experimental observations.

We should point out, that in the present report we focused our attention only on formation of amido and amido–amido compounds and their oligomers. Further HBr elimination reactions from amido–amido compounds will lead to amido–imido and imido–imido species and respective oligomers (see Scheme 1). Experimentally observed ions $MC_2N_2H_6^+$ and $M_2X_2C_2N_2H_6^+$ could be a daughter ions from these imido or amido–imido oligomers. Our preliminary results suggest that in contrast of the amido compounds, stability of imido oligomers increases with increase of the oligomerization degree n [19,21]. Detailed discussion of structures and stability of $\mathbf{AI_n}$, $\mathbf{I_n}$ and $\mathbf{II_n}$ compounds lies out of scope of the present report and will be presented in our future publications.

4. Conclusion

Complexes of group 13 metal halides with en of 2:1 composition upon heating undergo thermal decomposition. As was evidenced by mass spectrometry method, initial stage of the decomposition processes is hydrogen halide elimination. Decomposition is accompanied by formation of a variety of gaseous high molecular weight compounds. In particularly, formation of the carbon-free cubane-type clusters was experimentally evidenced. The abundance of the high molecular weight species decreases in order $AlBr_3 > AlI_3 > GaCl_3 > GaBr_3$. $AlBr_3$en$AlBr_3$ system exhibit maximal variety of the cluster species in vapors, for gallium containing systems only a few species have been observed.

Theoretical *ab initio* studies at B3LYP/LANL2DZ(d,p) level of theory have been performed for the series of the amido ring and cage oligomer compounds (M = Al;

X = Br). It is concluded, that amido and amido–amido oligomers are thermodynamically unstable with respect to dissociation into ring monomers. HBr elimination from the complex $AlBr_3 \cdot en \cdot AlBr_3$ with formation of monomeric amido and amido–amido compounds is strongly endothermic but it is entropically favorable. Nevertheless, according our theoretical predictions, gas phase HBr elimination reactions are too energetically demanding, suggesting that HBr elimination reactions take place in the condensed phase after the melting of the complex. Formation of carbon-free cubanes can be explained as a result of a pyrolytic process wich is accompanied by formation of gaseous HBr, H_2 and solid carbon.

Acknowledgements

A.Y.T. is grateful to the INTAS for the YS05-109-4196 fellowship and Russian Foundation for Basic Research for a travel Grant 06-03-42772. Service of the computer cluster of St. Petersburg State University is gratefully acknowledged.

Appendix A. Supplementary data

Supplementary data associated with this article can be found, in the online version, at doi:10.1016/j.jorganchem.2007.02.022.

References

[1] A.C. Jones, P. O'Brien, CVD of compound semiconductors. Precursor Synthesis, Development and Applications, VCH, Weinheim, 1997.
[2] A.Y. Timoshkin, H.F. Schaefer, Chem. Record 2 (2002) 319–338.
[3] E.A. Berezovskaya, A.Y. Timoshkin, T.N. Sevastianova, A.D. Misharev, A.V. Suvorov, H.F. Schaefer, J. Phys. Chem. B. 108 (2004) 9561–9563.
[4] A.Y. Timoshkin, A.V. Suvorov, A.D. Misharev, C. Trinh, Vestnik St. Peterb. Universiteta. Ser. 4 (Khim, Fiz.) N2 (2006) 37–45.
[5] A.Y. Timoshkin, E.A. Berezovskaya, A.V. Suvorov, A.D. Misharev, Russ. J. Gen. Chem. 75 (2005) 1173–1179.
[6] Gmelin Handbook of Inorganic Chemistry. Ga. Organogallium Compounds. 8th ed., Springer-Verlag, Berlin, 1987.
[7] F.C. Sauls, L.V. Interrante, Coord. Chem. Rev. 128 (1993) 193–207.
[8] J.E. Park, B.-J. Bae, Y. Kim, J.T. Park, I.-H. Suh, Organomet. 18 (1999) 1059–1067.
[9] T. Belgardt, J. Storre, A. Klemp, H. Gornitzka, L. Häming, H.-G. Schmidt, H.W. Roesky, J. Chem. Soc., Dalton Trans. (1995) 3747–3751.
[10] A.Y. Timoshkin, Coord. Chem. Rev. 249 (2005) 2094–2131.
[11] A.Y. Timoshkin, A.V. Suvorov, H.F. Bettinger, H.F. Schaefer, J. Am. Chem. Soc. 119 (1997) 5668–5678.
[12] A.Y. Timoshkin, H.F. Bettinger, H.F. Schaefer, J. Crystal Growth 222 (2001) 170–182.
[13] J. Frisch, G.W. Trucks, H.B. Schlegel, G.E. Scuseria, M.A. Robb, J.R. Cheeseman, J.A. Montgomery Jr., T. Vreven, K.N. Kudin, J.C. Burant, J.M. Millam, S.S. Iyengar, J. Tomasi, V. Barone, B. Mennucci, M. Cossi, G. Scalmani, N. Rega, G.A. Petersson, H. Nakatsuji, M. Hada, M. Ehara, K. Toyota, R. Fukuda, J. Hasegawa, M. Ishida, T. Nakajima, Y. Honda, O. Kitao, H. Nakai, M. Klene, X. Li, J.E. Knox, H.P. Hratchian, J.B. Cross, C. Adamo, J. Jaramillo, R. Gomperts, R.E. Stratmann, O. Yazyev, A.J. Austin, R. Cammi, C. Pomelli, J.W. Ochterski, P.Y. Ayala, K. Morokuma, G.A. Voth, P. Salvador, J.J. Dannenberg, V.G. Zakrzewski, S. Dapprich, A.D. Daniels, M.C. Strain, O. Farkas, D.K. Malick, A.D. Rabuck, K. Raghavachari, J.B. Foresman, J.V. Ortiz, Q. Cui, A.G. Baboul, S. Clifford, J. Cioslowski, B.B. Stefanov, G. Liu, A. Liashenko, P. Piskorz, I. Komaromi, R.L. Martin, D.J. Fox, T. Keith, M.A. Al-Laham, C.Y. Peng, A. Nanayakkara, M. Challacombe, P.M.W. Gill, B. Johnson, W. Chen, M.W. Wong, C. Gonzalez, J.A. Pople, Gaussian 03, Revision B. 05, Gaussian Inc., Pittsburgh, PA, 2003.
[14] A.D. Becke, J. Chem. Phys. 98 (1993) 5648–5652.
[15] C. Lee, W. Yang, R.G. Parr, Phys. Rev. B 37 (1988) 785–789.
[16] P.J. Hay, W.R. Wadt, J. Chem. Phys. 82 (1985) 270–283.
[17] A.Y. Timoshkin, A.V. Suvorov, H.F. Bettinger, H.F. Schaefer, J. Am. Chem. Soc. 121 (1999) 5687–5699.
[18] C. Trinh, A.Y. Timoshkin, G. Frenking, ChemPhysChem 8 (2007) 425–432.
[19] A.Y. Timoskin, H.F. Bettinger, H.F. Schaefer, Inorg. Chem. 41 (2002) 738–747.
[20] Z. Jiang, L.V. Interrante, Chem. Mater. 2 (1990) 436–439.
[21] A.Y. Timoskin, H.F. Schaefer, Inorg. Chem. 43 (2004) 3080–3089.
[22] NIST Standard Reference Database number 69, june 2005. NIST Chemistry webbook. <http://webbook.nist.gov/chemistry>.